Environmental Modelling & Software 59 (2014) 91–97

Contents lists available at ScienceDirect

Environmental Modelling & Software

journal homepage: www.elsevier.com/locate/envsoft

Identification of firefighter safety zones using lidar

Philip E. Dennison*, Gregory K. Fryer, Thomas J. Cova

Department of Geography and Center for Natural and Technological Hazards, University of Utah, 260 S Central Campus Dr., Salt Lake City, UT 84112, USA

ARTICLE INFO

Article history:
Received 17 January 2014
Received in revised form
12 May 2014
Accepted 21 May 2014
Available online 11 June 2014

Keywords:
Fire safety
Wildland fire
Safety zone
Flame height
Remote sensing

ABSTRACT

Safety zones protect wildland firefighters from dangerous heat exposure, and are separated from fuels by a safe separation distance (SSD) derived from flame height. In this study, we describe a model for automated identification of safety zones using decision rules based on lidar-measured vegetation height, flame height, and terrain slope. Inputs included lidar and orthoimage data collected over a study area in the southern Sierra Nevada, USA. Safety zones were required to be large enough to shelter 20 firefighters and two vehicles, and distance to the closest road was measured to determine ease of access. Safety zones comprised less than 0.5% of the study area at 4 m flame height (16 m SSD). As flame height increased, the number and size of safety zones decreased. This model provides a flexible framework for identification of safety zones, which should assist firefighters and reduce potential for injury and loss of life.

1. Introduction

Unanticipated fire behavior can place firefighters at risk of injury or death due to exposure to intense heat produced by fuel combustion (Alexander et al., 2012). Entrapment and burnover fatalities occur in situations where firefighters are unable to reach an adequate safety zone protected from fire. Establishing safety zones is essential for reducing risk of firefighter injury and fatality, since safety zones provide a buffer between personnel and the fire (Beighley, 1995). Firefighters are regularly trained to identify safety zones, and escape routes to safety zones, in advance of engaging in fire suppression activities (Gleason, 1991; National Wildfire Coordinating Group, 2014).

A safety zone is separated from fuels by a safe separation distance (SSD) needed to reduce radiative and convective heating to noninjurous levels (Butler, 2014). The size of a safety zone is determined based on the number of personnel and equipment requiring protection, and the area required for each (Butler and Forthofer, 2002). An idealized representation using a circular clearing places the safety zone at the center, with the SSD extending in all directions between the safety zone and fuels (Fig. 1).

Radiative energy transfer models have provided guidelines for SSD based on flame height or flame length, but have made multiple simplifying assumptions including flat terrain, uniform flame temperature and/or emissivity, and lack of convective heat transfer (Butler, 2014). Flame height is measured in the vertical dimension, while flame length may be longer due to tilting of the flame by wind and slope. Based on a maximum heat threshold of 7 kWm^{-2} for firefighters wearing protective clothing, Butler and Cohen (1998) modeled the relationship between flame height and SSD. They proposed a guideline that SSD should exceed a minimum of four times flame height to provide a distance safe from heat exposure. Butler and Forthofer (2002) used an improved radiative energy transfer model to account for a curved flame sheet tilted toward the safety zone with a vertical temperature gradient. This improved model, along with measurements from experimental crown fires (Butler and Cohen, 2000), maintained the four-times-flame height guidance. Rossi et al. (2011) demonstrated that minimum SSDs from flame fronts are dependent on modeled flame temperature, with a cooler assumed temperature producing distances in the 2–3 times flame length range and a hotter assumed temperature producing distances up to 10 times flame length. The BehavePlus fire modeling system (Andrews, 2009) has incorporated guidelines from Butler and Cohen (1998) to provide a SAFETY module for calculating minimum SSD from fire. Flame length calculated from a surface fire model (Albini, 1976; Byram, 1959) is assumed to represent worst case flame height. The National Wildfire Coordinating Group (NWCG) uses a four times flame height guideline for SSD, but notes that safety zones downwind or upslope from fire may require a larger SSD (National Wildfire Coordinating Group, 2014).

Safety zones are typically determined on-site using minimum safety zone size and SSD requirements. Firefighter perception of

* Corresponding author. Room 270. Tel.: +1 801 585 1805.
E-mail address: dennison@geog.utah.edu (P.E. Dennison).

http://dx.doi.org/10.1016/j.envsoft.2014.05.017
1364-8152/

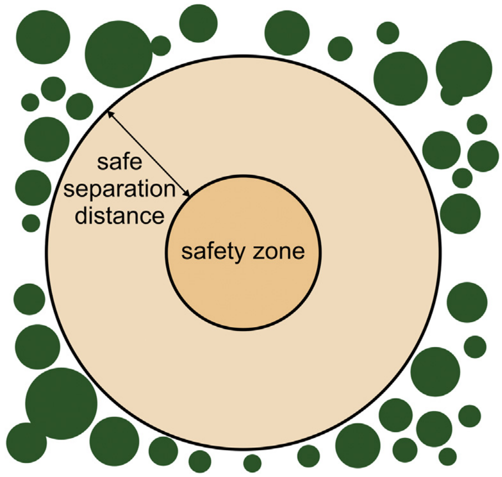

Fig. 1. A safety zone determined using a safe separation distance from the closest trees, possessing an area large enough to contain the protected personnel and equipment. After Butler and Forthofer (2010).

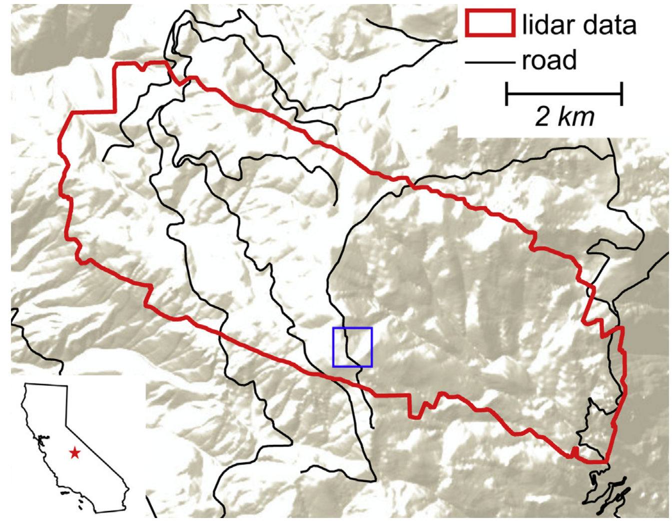

Fig. 2. Study area in Sierra National Forest, California, USA. The square indicates the subset area shown in Fig. 3 and Figs. 8–10.

SSD in given conditions may be flawed; Steele (2000) found that firefighters shown a fuel photograph series had widely ranging estimates of minimum SSD. Detailed information on the geographic distribution of vegetation, provided by high resolution remote sensing, may permit automated identification of safety zones over large areas well in advance of wildfire occurrence. In this paper, we demonstrate a spatial model capable of determining safety zones using lidar and orthoimage inputs. A series of decision rules can be used to adjust parameters such as flame height and maximum terrain slope. Outputs such as safety zone size and distance to the closest road can aid in determining whether modeled safety zones are suitable for firefighter protection. This model provides an automated means for identifying safety zones that may assist firefighter decision making and reduce risk of firefighter injury and fatality.

2. Methods

2.1. Data

A study area in Sierra National Forest, California, USA was selected based on lidar data availability (Fig. 2). Vegetation in the study area is predominantly mixed conifer forest, typically comprised of Jeffrey pine (*Pinus jeffreyi*), ponderosa pine (*Pinus ponderosa*), sugar pine (*Pinus lambertiana*), incense cedar (*Calocedrus decurrens*), and white fir (*Abies concolor*). Lodgepole pine (*Pinus contorta*) and red fir (*A. magnifica*) dominate at higher elevation. Meadows with herbaceous vegetation and shrub cover are widely dispersed.

Airborne lidar uses laser pulses to measure the range between the aircraft and the Earth's surface. Multiple returns from the same pulse can be recorded to determine the elevation of both the vegetation canopy and ground surface. Discrete return lidar data were collected over a 22 km^2 area capturing part of the Southern Sierra Critical Zone Observatory in August 2010 by the National Center for Airborne Laser Mapping (Anderson et al., 2012). The data were collected with an average point density of approximately 11.7 points per m^2. The point cloud was processed to 1 m gridded products made available through the OpenTopography Project. A "first return" digital surface model (DSM) captures the highest elevation of the points within each grid cell (Fig. 3c). A corresponding 1 m "bare earth" digital terrain model (DTM) (Fig. 3b) is created by interpolating the lowest elevation returns in the point cloud (Guo et al., 2010). For vegetated surfaces, the first return DSM represents the absolute elevation of the upper vegetation canopy (Clark et al., 2004; Lefsky et al., 2002). The bare earth DTM was subtracted from the first return DSM to provide vegetation height. Slope over a 15 m by 15 m window was calculated using the bare earth DTM (Fig. 3d). Mean slope within the study area was 15°. Color infrared digital imagery was acquired over the study area by the National Agriculture Imagery Program (NAIP) in summer 2010. These data are orthorectified to create 1 m spatial resolution composites with near infrared (NIR), red, green, and blue bands (Fig. 3a). Nearest neighbor resampling was used to align the orthoimagery to the lidar gridded data.

2.2. Safety zone requirements

A transect across the lidar subset in Fig. 3 demonstrates how the first return DSM and bare earth DTM capture gaps between vegetation canopies that can potentially be used as safety zones (Fig. 4). Vegetation heights exceeding a threshold can be buffered by an SSD determined by flame height. Once the SSD is accounted for, the resulting safety zone must be large enough to shelter both personnel and equipment (Fig. 1). As the number of firefighters and vehicles change, the minimum safety zone size will also change. The BehavePlus fire modeling system provides guidelines for the minimum area required by both personnel and heavy equipment (Andrews, 2009). Approximately five square meters (50 square feet) is recommended for each firefighter to have space to deploy a fire shelter, which if becomes necessary, would make the safety zone a "deployment zone". Approximately 28 square meters (300 square feet) is given as an average area needed for heavy equipment (Andrews, 2009). Examples of heavy equipment include trucks, dozers, and engines. For this study, we assumed a crew of 20 firefighters accompanied by two pieces of heavy equipment. Using these assumptions, any safety zone was required to contain a minimum of 156 m^2. This should be regarded as the minimum size of a safety zone, with no safety margin applied. Safety zones larger than this minimum would provide additional protection.

2.3. Safety zone modeling

Decision trees were used to determine whether each 1 m grid cell was suitable as a part of a safety zone. Simplified decision trees illustrating this process are shown in Fig. 5. An initial decision tree splits cells into "buffered cell" and "unbuffered cell" categories (Fig. 5a). Buffered cells are considered to be tall fuels that are likely to produce tall flame heights. These cells are buffered by a distance of four times the expected maximum flame height based on NWCG guidelines (National Wildfire Coordinating Group, 2014), and cannot be used as part of a safety zone. A second decision tree splits the unbuffered cells into "safe cell" and "unsafe cell" categories (Fig. 5b). The primary decision rule is whether the distance to the closest buffered fuel cell is less than or greater than four times the expected maximum flame height (Fig. 5b). Additional criteria, such as slope and minimum safety zone size, can be used to further refine safety zones.

Decision trees were implemented in the Interactive Data Language (IDL), version 8.2 (Exelis Visual Information Solutions, Boulder, Colorado, USA). The coregistered first return DSM, bare earth DTM, terrain slope, and orthoimage data were read into memory and used to calculate vegetation height and normalized difference vegetation index (NDVI). A more complex rule set was implemented to identify safety zones for the study area (Table 1). All decision points were determined empirically, but are easily adjustable based on expert knowledge. For the first decision tree, the vegetation height grid was used as described above. A vegetation height threshold of 1 m was used to separate buffered cells containing tree and tall shrub fuels from unbuffered cells containing low or no fuels. Shorter fuels in the 0.2–1 m range were excluded from safety zones in a step described below, but were not buffered. In some clearings, we found that single, isolated trees were classified as buffered cells and resulted in reduced safety zone size. A potential safety zone containing a small number of hazardous trees may be made safe by felling those trees. To increase safety zone size in situations where site fuel treatment may be possible, a second decision rule was created to reduce the number of buffered cells assigned to isolated trees (Table 1). A 25 m kernel was applied to the

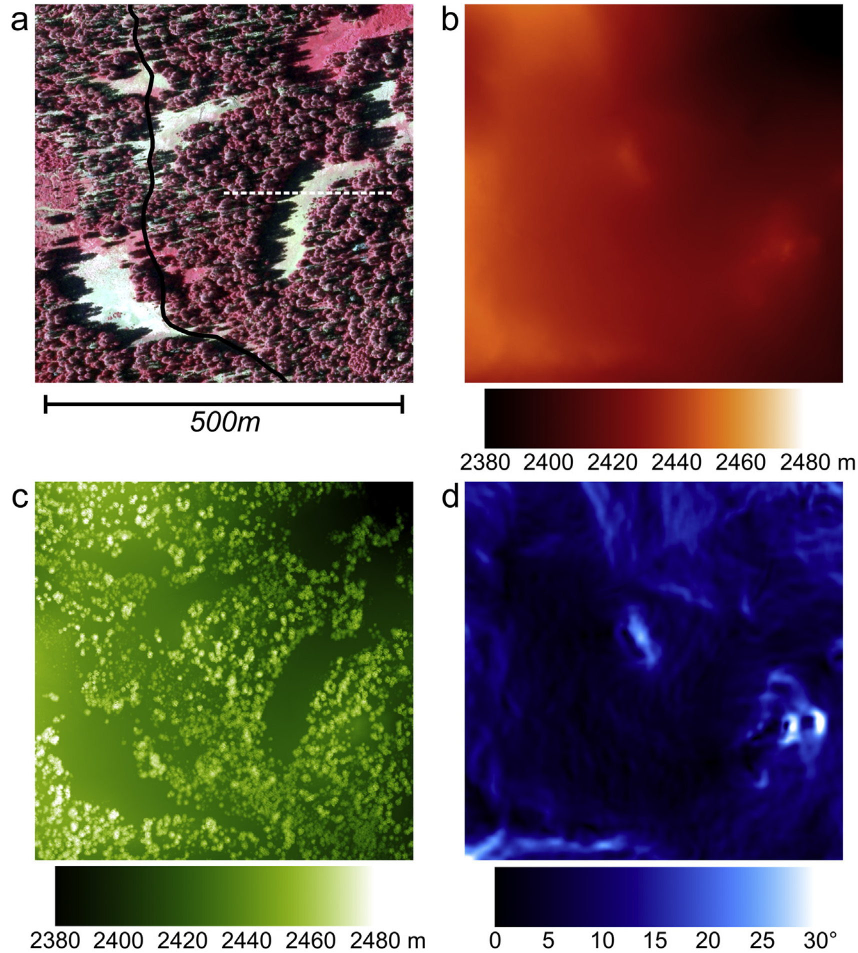

Fig. 3. Inputs used for the safety zone model, shown for the subset of the larger study area in Fig. 2. (a) Digital color infrared orthoimagery. The black line is a digitized road crossing the subset. The dashed white line indicates the position of the transect shown in Fig. 4. (b) Lidar bare earth DTM. (c) Lidar first return DSM. (d) Slope calculated from the bare earth DTM. (For interpretation of the references to color in this figure legend, the reader is referred to the web version of this article.)

vegetation height grid, and the percentage of cells in the kernel exceeding the 1 m vegetation height threshold was calculated and assigned to the cell. If less than 10% of the cells in the kernel exceeded the vegetation height threshold, then tree cover was considered sparse and the cell was assigned to the unbuffered category. Otherwise, with both the cell vegetation height exceeding 1 m and more than 10% of the kernel exceeding 1 m, the cell was assigned to the buffered category. Safety zones calculated using no kernel and safety zones calculated using a 25 m kernel were compared.

Additional decision rules for the second decision tree (Table 1) were applied to unbuffered cells determined using the first tree. In an actual fire scenario, flame length would be calculated from a fire behavior modeling system such as BehavePlus (Andrews, 2009) and used as flame height. In such cases, the estimate or prediction of flame length is based on a fuel model and environmental characteristics (wind speed and direction, fuel moisture, etc.). Separate safety zone model runs used a maximum expected flame height that ranged from 2 to 14 m in 1 m increments. Fire with 1 m flame height was assumed to be suppressible using hand tools and/or equipment (National Wildfire Coordinating Group, 2014). Distance to the closest buffered fuel cell was specified as four times flame height based on NWCG guidelines (National Wildfire Coordinating Group, 2014), so the minimum SSD between safety zone cells and buffered fuel cells ranged between 8 m and 56 m. No viable safety zones were found for flame heights longer than 14 m using the four times flame height SSD. The four times flame height SSD is modifiable to provide an additional safety margin if necessary.

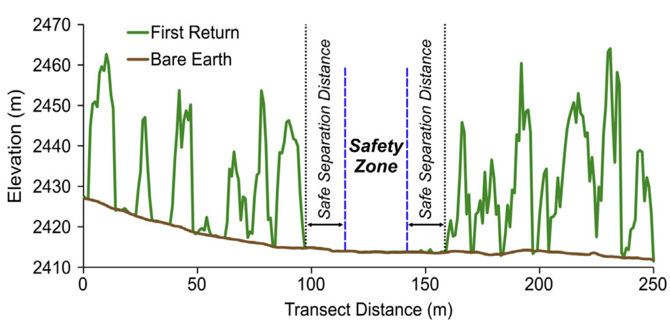

Fig. 4. A 250 m profile across a transect of the subset shown in Fig. 3. Note that scaling on the *y*-axis is exaggerated to improve visibility of vegetation height.

Subsequent decision rules were used to exclude individual unbuffered cells from safety zones. Safe cells were required to have a slope less than 10°, since slopes can have increased convective heat exposure (Butler et al., 2010), guidelines based on SSD models assume flat slopes (Butler, 2014), and equipment and personnel can have difficulty traveling up steeper slopes (Alexander et al., 2013; Baxter et al., 2004). Vegetation height was combined with NDVI to exclude unbuffered cells with vegetation having heights between 0.2 m and 1 m. NDVI (Rouse et al., 1973) is calculated as:

$$NDVI = \frac{NIR - red}{NIR + red}$$

using the orthoimage NIR and red bands. Since the orthoimage used scaled brightness values, NDVI values typically calculated from reflectance data did not apply and an empirical threshold distinguishing green vegetation was required. Cells with both vegetation height exceeding 0.2 m and NDVI exceeding 0.1 were considered likely to have shrubby vegetation cover based on photointerpretation of the orthoimage, and were excluded from being safe cells. Finally, the number of contiguous safe cells, counted using four neighbors for each cell, was required to exceed 156 m^2 to create a safety zone. Distance to the road shown in Fig. 3a was also calculated for each cell, but not used as a decision rule.

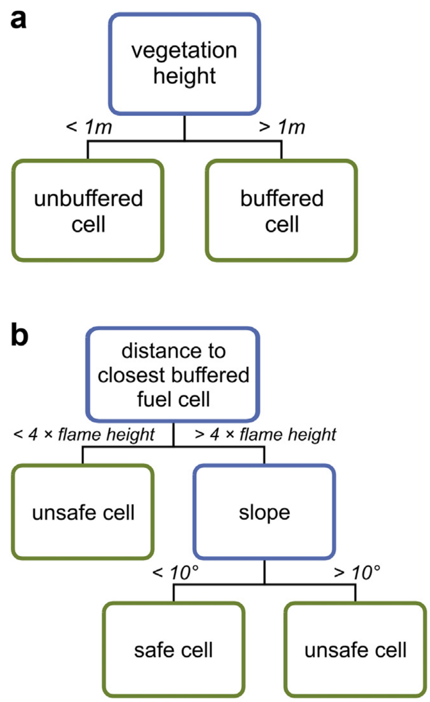

Fig. 5. (a) Shows a simple decision rule for separating buffered cells containing tall vegetation from unbuffered cells. Unbuffered cells from (a) are used in (b) to separate safe cells that can comprise a safety zone from unsafe cells. More complete decision rules used in the case study are described in Table 1.

3. Results

Most of the 2.2 km^2 covered by lidar data was found to be unsuitable for use as safety zones (Fig. 6). For a flame height of 4 m and no kernel used to exclude isolated trees from being buffered cells, 42 safety zones comprised less than 0.2% of the study area (Table 2). As flame height increased, the number of safety zones capable of containing 20 firefighters and 2 pieces of heavy equipment decreased. Using a 25 m kernel to exclude isolated trees approximately doubled the number of safety zones found and more than doubled the total area of all safety zones (Table 3). The 75 safety zones found at 4 m flame height and the 5 safety zones found at 10 m flame height using the 25 m kernel are shown in Fig. 6. The average size of safety zones was greater when the kernel was used, increasing from 930 m^2 to 1176 m^2 for 4 m flame height. As flame heights increased, the average size of safety zones decreased due to the longer SSD.

An example of a clearing with isolated trees that was affected by the application of a 25 m kernel for screening vegetation height is shown in Fig. 7. The arrow points towards a single tall tree; a few additional isolated, shorter trees are obscured by the green line. The blue polygons denote two safety zones found using no kernel, exceeding 156 m^2 each. The clearing is split into two safety zones because the isolated trees are buffered by a 16 m SSD, resulting in smaller safety zones. The single green polygon is the safety zone resulting from using the 25 m kernel to prevent isolated trees from being classified as buffered cells. The unbuffered "hole" in the polygon created by the tree itself has been omitted for clarity. The green polygon still maintains an SSD from denser clumpings of tree canopies, such as at the right edge of the clearing. Using safety zones created from both no kernel and 25 m kernel model runs could allow separation of primary safety zones from those needing improvement. All further examples use the 25 m kernel to exclude isolated trees from use as buffered cells.

Increasing flame height resulted in fewer areas meeting the minimum size requirement for selection as a safety zone. Fig. 8 displays safety zones in the same subset shown in Fig. 3. At 4 m flame height, effectively a 16 m distance from the forest edge, a total of six safety zones were found within the subset. The portions of these clearings not labeled as safety zones were too narrow, too steep, and/or vegetation cover was too tall according to the second decision tree. At 6 m flame height, four of the safety zones disappear or become too small to meet the 156 m^2 threshold. The remaining two safety zones shrink due to the increased SSD of 24 m.

Area and access are important considerations for selecting potential safety zones. Spatial modeling allows determination of both the area within each safety zone and distance to the closest road (Fig. 9). For the six safety zones identified within the subset at a 4 m flame height, three are accessible within a short distance of the road. Two of these safety zones are relatively small, at 345 m^2 and 628 m^2, and would not remain safety zones for higher flame heights. The safety zone in the lower left corner of the subset has both a short distance to the closest road, and a size many times that required for a flame height of 4 m. The three safety zones on the right side of the subset, while having sufficient size, may be difficult to access because of longer distances from the road and intervening terrain.

Combining the safety zones across all flame heights provides insight into the maximum flame height to which each clearing can be exposed to while still serving as a safety zone (Fig. 10). Portions of clearings not designated as safety zones represent unbuffered cells that were excluded due to size, slope, or vegetation height/NDVI criteria. The four clearings at the top of the subset are suitable for flame heights up to 4 or 5 m. Two clearings are sufficient for 6 m flame heights, but only the lower left clearing in Fig. 10 is large enough to include area for 20 firefighters and 2 pieces of heavy equipment at 10 m flame height. Over the entire study area, only 5 clearings were sufficiently large enough at 10 m flame height (Table 3), and 2 of these clearings are likely to need some improvement to be suitable (Table 2). No safety zones were found within the study area for flame heights in excess of 14 m.

4. Discussion

Automated identification of safety zones using lidar data is most likely to be helpful to firefighters engaged in indirect attack ahead of or flanking a wildfire. Flame heights may be too high, and fire spread too rapid, to engage in direct suppression. Indirect attack often has firefighters creating fuel breaks hundreds or thousands of meters away from the fire front, but firefighters need to be prepared to evacuate to a safety zone if fire spread threatens their position (Beighley, 1995). For a single incident, safety zones could be determined each day using a maximum flame height modeled by a fire behavior analyst. Safety zones could also be mapped ahead of fire season based on available lidar data and a range of potential flame heights. In either use, safety zones identified based on remotely sensed data must still be verified in the field. Vegetation cover may change over time, and lidar and orthoimagery may not reveal hazards present within a prospective safety zone.

Decision rules could be used to rate safety zone suitability based on remotely sensed attributes. For example, safety zones with lower vegetation height or greener vegetation cover (as assessed through NDVI) could be ranked above safety zones with higher vegetation height and senesced vegetation cover. Automated mapping of safety zones ahead of fire season provides opportunities for safety zone improvement. Safety zones that are nearly of sufficient size for expected flame heights or that might have isolated trees or shrubs could be identified. These sub-standard safety

Table 1
Safety zone decision rules.

Parameter	Case study decision point	Rule description
First tree		
Vegetation height	1 m	Vegetation height is the difference between the lidar first return DSM and the bare earth DTM. A vegetation height threshold separates buffered cells (e.g. trees) from lower height unbuffered cells.
Percent of kernel above vegetation height threshold	10%	A 25 m kernel is used to screen out small areas above the vegetation height threshold (1 m) that are surrounded by heights below the vegetation height threshold. This preserves safety zones that may need treatment before use, like clearings with a single tree. If less than 10% of the kernel is above 1 m, then the cell becomes unbuffered rather than buffered.
Second tree		
Distance to closest buffered fuel cell	8–56 m (4 × flame height)	Safe cells must have an SSD at least four times the flame height away from buffered cells, as determined by the vegetation height and percent of kernel above vegetation height threshold parameters.
Slope	10°	Cell slope, calculated from the bare earth DTM, is limited to below 10° to be a safe cell. Steep slopes may increase heat exposure, go beyond the assumptions of radiative energy transfer models used to calculate SSD, and may be more difficult to access.
Vegetation height AND NDVI	20 cm, 0.1	Fuels shorter than 1 m may not be suitable for sheltering. Fuels taller than 20 cm and with a Normalized Difference Vegetation Index greater than 0.1 are excluded from being safe cells, but are not buffered based on flame height.
Contiguous area	156 m^2	The total area of contiguous safe cells must exceed a minimum size based on the number of personnel and equipment to qualify as a safety zone. 20 firefighters and 2 vehicles were assumed.
Distance to closest road	not used	Distance between each safe cell and the nearest cell classified as road should not exceed a maximum value to facilitate travel to the safety zone.

zones could then be improved by clearing additional area well before fire threatens. Once safety zones are known, access can be assessed in advance and improved if necessary.

Our model utilized one SSD based on a single expected maximum flame height, but flame height could vary across the study area. Improvements to the model could incorporate variable flame heights through two different methods. A combination of lidar vegetation height and orthoimagery could be used to map fuel models at a fine spatial scale. Expected flame heights for each fuel model could be determined (Zárate et al., 2008), which would then be used to vary the SSD for each fuel type. Lidar vegetation height itself may offer an alternative method for incorporating flame height. Current fire behavior models do not take advantage of continuous vegetation height and density as input parameters, but flame height is likely to be correlated with these parameters under a given set of weather conditions. As an alternative to incorporating spatially variable flame heights, radiative transfer modeling could

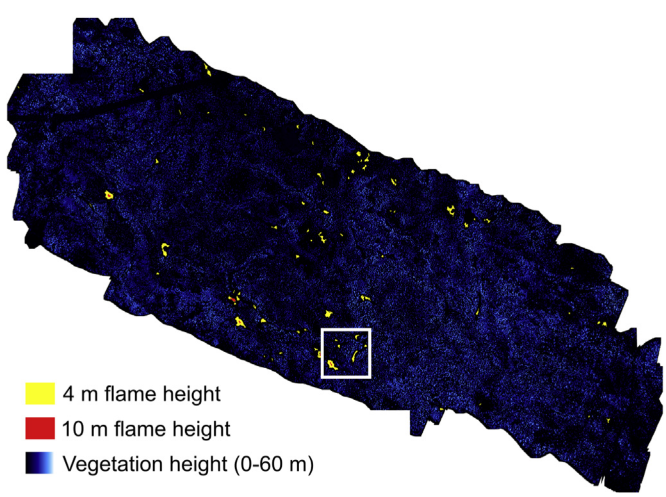

Fig. 6. Study area safety zones for 4 m and 10 m flame height, using the 25 m kernel to exclude isolated trees. The white box indicates the area shown in Fig. 3 and Figs. 8–10. (For interpretation of the references to colour in this figure legend, the reader is referred to the web version of this article.)

Table 2
Safety zone statistics for the no kernel model runs.

Flame height	4 m	6 m	10 m
Number of safety zones	42	13	3
Total area (m^2)	39,041	11,884	1637
% of study area	0.18%	0.05%	0.01%

Table 3
Safety zone statistics for the 25 m kernel model runs.

Flame height	4 m	6 m	10 m
Number of safety zones	75	30	5
Total area (m^2)	88,168	30,431	3544
% of study area	0.40%	0.14%	0.02%

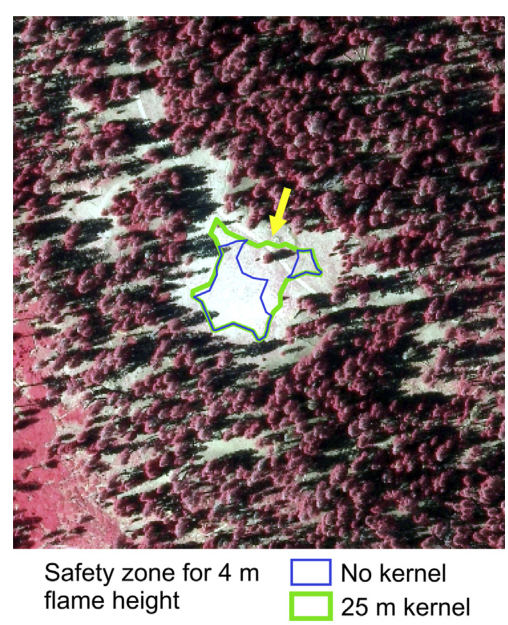

Fig. 7. A comparison of safety zones for a clearing with one large tree, indicated by the arrow.

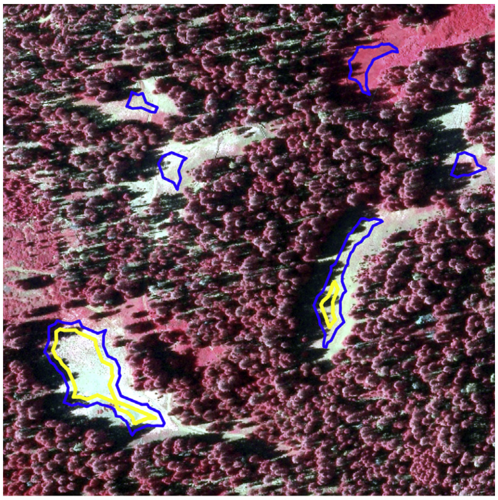

Fig. 8. Safety zones calculated for 4 and 6 m flame heights.

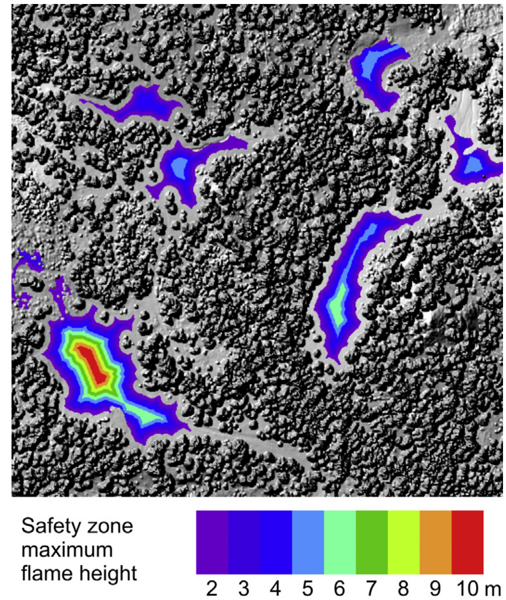

Fig. 10. The maximum flame height that still permits each cell to be part of a safety zone, with the hillshaded first return DSM shown in the background.

be used to directly estimate maximum heat exposure in each grid cell across the landscape, although flame width, depth, and duration would also need to be assumed (Butler and Forthofer, 2002; Butler and Cohen, 1998; Rossi et al., 2011). All of these methods could potentially reveal additional safety zones not captured by a single flame height, but may also result in undesirable increases in model complexity and run time.

Decision rules used for this model were empirically determined, and do not provide optimum separability between safety zone cells and unsafe cells. The framework presented here is flexible and could utilize a variety of lidar and orthoimage inputs. Variables capturing topographic position may be necessary to exclude safety zones from being placed on hilltops and saddles, which are vulnerable to rapid upslope fire spread due to enhanced wind effects. Decision rules and points were based on a study area in Sierra Nevada mixed conifer forest, but these decision rules may perform more poorly in different regions such as lower height chaparral in southern California. Classification And Regression Tree (CART) methods (De'ath and Fabricius, 2000) may aid in determining optimum decision rules that are functional across a wide range of fuel types.

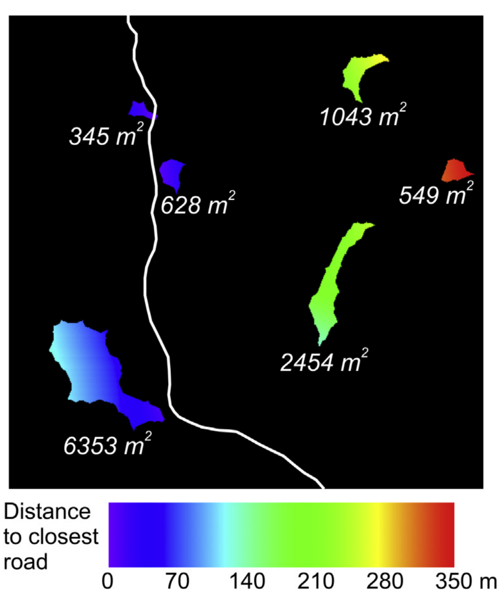

Fig. 9. Safety zones calculated for 4 m flame height. Distance to the road (shown as a white line) is indicated for cells in each safety zone. Italicized numbers represent the total area of each safety zone.

Our model did calculate distance to the closest road, but did not address the issue of travel time. Travel time varies according to distance, slope, and vegetation type (Alexander et al., 2013; Baxter et al., 2004). Steep slopes and dense vegetation will make safety zones more difficult to access, regardless of distance. Beyond roads, accessibility can be an issue for many types of equipment, which could force travel on foot and further impact travel time. Natural barriers such as steep slopes or rock faces may render some safety zones inaccessible on foot or in vehicles. Travel time to safety zones and accessibility, both on foot and using vehicles (Fryer et al., 2013), should be included in future safety zone modeling.

Lidar identification of safety zones also has potential for use in the wildland urban interface (WUI). Lidar data can be utilized for mapping structures (Ma, 2005; Warnick et al., 2005; Zhang et al., 2006), and buffering structures using expected flame height could be used to determine whether a structure has sufficient defensible space surrounding it. Based on defensible space and accessibility, WUI structures that are suitable for shelter actions (Cova et al., 2009) may be distinguishable.

5. Conclusions

In this paper we present a spatial model capable of identifying safety zones based on expected maximum flame height. Decision trees allow consideration of distance from fuels and roads, vegetation height, and slope, providing a quantitative assessment of safety zone suitability. Safety zones were found to comprise a small fraction of a mixed conifer forest study area, and decreased in size and number as flame height increased. Use of a 25 m kernel to eliminate isolated trees as buffered fuel cells resulted in larger, more numerous safety zones, and could be used to highlight potential safety zones needing improvement. Safety zone size and distance from roads are readily available using spatial modeling, and this type of model could be further developed to incorporate travel time to safety zones.

Lidar provides a powerful tool for high resolution separation of dangerous fuels from clearings that may serve as safety zones. While this model provides a flexible framework for safety zone identification, its primary limitation is its reliance on lidar data. Airborne, small footprint lidar data are only available for a small fraction of fire prone lands. Lidar data availability could greatly improve with national-scale programs similar to those for the acquisition of aerial imagery (e.g. NAIP). A national lidar program coordinating multiple federal agencies has been proposed for the United States (Stoker et al., 2008), and several US states have lidar acquisition programs. Greatly increased lidar availability in the near future could make regional scale safety zone mapping feasible.

Acknowledgments

We thank B. Butler and three anonymous reviewers for their insightful comments. This research was supported by National Science Foundation CMMI-IMEE grant number 1100890. Lidar data were provided by the OpenTopography Facility with support from NSF award numbers 1226353 & 1225810.

References

Albini, F.A., 1976. Estimating Wildfire Behavior and Effects. General Technical Report INT-30. US Department of Agriculture, Forest Service, Intermountain Forest and Range Experiment Station, Ogden, UT.
Alexander, M., Baxter, G., Dakin, G., 2013. How much time does it take for a wildland firefighter to reach a safety zone? Wildfire 22 (4), 12–13.
Alexander, M.E., Mutch, R.W., Davis, K.M., Bucks, C.M., 2012. Wildland fires: dangers and survival. In: Auerbach, P.S. (Ed.), Wilderness Medicine, sixth ed. Elsevier, Philadelphia, pp. 240–280.
Anderson, S., Qinghua, G., Parrish, E., 2012. Snow-on and Snow-off LiDAR Point Cloud Data and Digital Elevation Models for Study of Topography, Snow, Ecosystems and Environmental Change at Southern Sierra Critical Zone Observatory, California. Southern Sierra CZO, University of California at Merced http://dx.doi.org/10.5069/G9BP00QB.
Andrews, P.L., 2009. BehavePlus Fire Modeling System, Version 5.0: Variables. General Technical Report RMRS-GTR-213WWW Revised. Department of Agriculture, Forest Service, Rocky Mountain Research Station, Fort Collins, CO.
Baxter, G., Alexander, M., Dakin, G., 2004. Travel Rates of Alberta Wildland Firefighters Using Escape Routes on a Moderately Steep Slope. Forest Engineering Research Institute of Canada, Point-Claire, QC and Vancouver, BC.
Beighley, M., 1995. Beyond the safety zone: creating a margin of safety. Fire Manag. Notes 55 (4), 21–24.
Butler, B., 2014. Wildland firefighter safety zones: a review of past science and summary of future needs. Int. J. Wildland Fire 23 (3), 295–308.
Butler, B., Cohen, J., 2000. Field verification of a firefighter safety zone model. In: Butler, B., Shannon, K. (Eds.), 4th International Wildland Fire Safety Summit. International Association of Wildland Fire, Edmonton, AB, pp. 54–61.
Butler, B., Forthofer, J., 2002. Get into the zone. Wildfire 11 (5), 16–22.
Butler, B., Forthofer, J., 2010. Wildland Firefighter Safety Zones. http://www.firemodels.org/downloads/behaveplus/tutorials/Modeling/21_SafetyZoneSize/Butler_and_Forthofer_2002_S390Attachment.pdf.
Butler, B., Forthofer, J., Shannon, K., Jimenez, D., Frankman, D., 2010. The effect of terrain slope on firefighter safety zone effectiveness. In: Wade, D.D., Robinson, M.L. (Eds.), 3rd Fire Behavior and Fuels Conference. International Association of Wildland Fire, Spokane, Washington, USA.
Butler, B.W., Cohen, J.D., 1998. Firefighter safety zones: a theoretical model based on radiative heating. Int. J. Wildland Fire 8 (2), 73–77.
Byram, G.M., 1959. Combustion of forest fuels. In: Davis, K.P. (Ed.), Forest Fire: Control and Use. McGraw-Hill, New York, NY, pp. 61–89.
Clark, M.L., Clark, D.B., Roberts, D.A., 2004. Small-footprint lidar estimation of sub-canopy elevation and tree height in a tropical rain forest landscape. Remote Sens. Environ. 91 (1), 68–89.
Cova, T.J., Drews, F.A., Siebeneck, L.K., Musters, A., 2009. Protective actions in wildfires: evacuate or shelter-in-place? Nat. Hazards Rev. 10 (4), 151–162.
De'ath, G., Fabricius, K.E., 2000. Classification and regression trees: a powerful yet simple technique for ecological data analysis. Ecology 81 (11), 3178–3192.
Fryer, G.K., Dennison, P.E., Cova, T.J., 2013. Wildland firefighter entrapment avoidance: modelling evacuation triggers. Int. J. Wildland Fire 22 (7), 883–893.
Gleason, P., 1991. LCES – a key to safety in the wildland fire environment. Fire Manag. Notes 52 (4), 9.
Guo, Q., Li, W., Yu, H., Alvarez, O., 2010. Effects of topographic variability and lidar sampling density on several DEM interpolation methods. Photogrammetric Eng. Remote Sens. 76 (6), 701–712.
Lefsky, M.A., Cohen, W.B., Parker, G.G., Harding, D.J., 2002. Lidar remote sensing for ecosystem studies: lidar, an emerging remote sensing technology that directly measures the three-dimensional distribution of plant canopies, can accurately estimate vegetation structural attributes and should be of particular interest to forest, landscape, and global ecologists. BioScience 52 (1), 19–30.
Ma, R., 2005. DEM generation and building detection from lidar data. Photogrammetric Eng. Remote Sens. 71 (7), 847–854.
National Wildfire Coordinating Group, 2014. Incident Response Pocket Guide. PMS 461. http://www.nwcg.gov/pms/pubs/pms461/pms461.pdf.
Rossi, J.L., Simeoni, A., Moretti, B., Leroy-Cancellieri, V., 2011. An analytical model based on radiative heating for the determination of safety distances for wildland fires. Fire Saf. J. 46 (8), 520–527.
Rouse, J., Haas, R., Schell, J., Deering, D., 1973. Monitoring vegetation systems in the Great Plains with ERTS. In: Freden, S., Mercanti, E., Becker, M. (Eds.), Third Earth Resources Technology Satellite Symposium. NASA, Washington, DC, pp. 309–317.
Steele, J., 2000. Effective firefighter safety zone size: a perception of firefighter safety. In: Butler, B., Shannon, K. (Eds.), 4th International Wildland Fire Safety Summit. International Association of Wildland Fire, Edmonton, AB, pp. 171–177.
Stoker, J., Harding, D., Parrish, J., 2008. The need for a national lidar dataset. Photogrammetric Eng. Remote Sens. 74, 1066–1068.
Warnick, R., Finco, M., Laes, D., Jarvis, B., Brewer, K., 2005. Mapping wildland-urban interface structures using LIDAR and High-Resolution Digital Orthophotos. In: EastFIRE Conference: Wildland Fire Research in the Eastern United States, pp. 11–23.
Zárate, L., Arnaldos, J., Casal, J., 2008. Establishing safety distances for wildland fires. Fire Saf. J. 43 (8), 565–575.
Zhang, K., Yan, J., Chen, S.-C., 2006. Automatic construction of building footprints from airborne LIDAR data. Geosci. Remote Sensing, IEEE Trans. 44 (9), 2523–2533.